A Pilot Study of Diffusion-Weighted MRI in Patients Undergoing Neoadjuvant Chemoradiation for Pancreatic Cancer

Kyle C. Cuneo[*,‡‡], Thomas L. Chenevert[†],
Edgar Ben-Josef[*,1], Mary U. Feng[*],
Joel K. Greenson[‡], Hero K. Hussain[†],
Diane M. Simeone[§], Matthew J. Schipper[¶],
Michelle A. Anderson[#], Mark M. Zalupski[**],
Mahmoud Al-Hawary[†], Craig J. Galban[†,††],
Alnawaz Rehemtulla[*], Felix Y. Feng[*],
Theodore S. Lawrence[*] and Brian D. Ross[†]

[*]Department of Radiation Oncology, University of Michigan, Ann Arbor, MI; [†]Department of Radiology, University of Michigan, Ann Arbor, MI; [‡]Department of Pathology, University of Michigan, Ann Arbor, MI; [§]Department of Surgery, University of Michigan, Ann Arbor, MI; [¶]Department of Statistics, University of Michigan, Ann Arbor, MI; [#]Department of Medicine-Gastroenterology, University of Michigan, Ann Arbor, MI; [**]Department of Medicine-Oncology, University of Michigan, Ann Arbor, MI; [††]Department of Biomedical Engineering, University of Michigan, Ann Arbor, MI; [‡‡]Department of Radiation Oncology, Ann Arbor Veterans Affairs Hospital, Ann Arbor, MI

Abstract

PURPOSE: In the current study we examined the ability of diffusion MRI (dMRI) to predict pathologic response in pancreatic cancer patients receiving neoadjuvant chemoradiation. *METHODS:* We performed a prospective pilot study of dMRI in patients with resectable pancreatic cancer. Patients underwent dMRI prior to neoadjuvant chemoradiation. Surgical specimens were graded according to the percent tumor cell destruction. Apparent diffusion coefficient (ADC) maps were used to generate whole-tumor derived ADC histogram distributions and mean ADC values. The primary objective of the study was to correlate ADC parameters with pathologic and CT response. *RESULTS:* Ten of the 12 patients enrolled on the study completed chemoradiation and had surgery. Three were found to be unresectable at the time of surgery and no specimen was obtained. Out of the 7 patients who underwent pancreaticoduodenectomy, 3 had a grade III histopathologic response (>90% tumor cell destruction), 2 had a grade IIB response (51% to 90% tumor cell destruction), 1 had a grade IIA response (11% to 50% tumor cell destruction), and 1 had a grade I response (>90% viable tumor). Median survival for patients with a grade III response, grade I-II response, and unresectable disease were 25.6, 18.7, and 6.1 months, respectively. There was a significant correlation between pre-treatment mean tumor ADC values and the amount of tumor cell destruction after chemoradiation with a Pearson correlation coefficient of 0.94 ($P = .001$). Mean pre-treatment ADC was 161×10^{-5} mm^2/s (n = 3) in responding patients (>90% tumor cell destruction) compared to 125×10^{-5} mm^2/s (n = 4) in non-responding patients (>10% viable tumor). CT imaging showed no significant change in tumor size in responders or non-responders. *CONCLUSIONS:* dMRI may be useful to predict response to chemoradiation in pancreatic cancer. In our study, tumors with a low ADC mean value at baseline responded poorly to standard chemoradiation and would be candidates for intensified therapy.

Address all correspondence to: Kyle C. Cuneo, MD.
[1] E.B.J. is now affiliated with the Department of Radiation Oncology at the University of Pennsylvania, Philadelphia, PA.

1. Introduction

The majority of patients with pancreatic cancer present with unresectable locally advanced disease. Standard of care therapy for locally advanced pancreatic cancer includes a combination of chemotherapy and radiation therapy [1]. A challenge in the management of pancreatic cancer is the early assessment of treatment response. Given the considerable toxicity of chemoradiation, this knowledge would be useful for selecting the most appropriate therapy for an individual patient.

Computed tomography detected responses in pancreatic cancer are slow and infrequent after chemoradiation [2–4] and underestimate the effectiveness of neoadjuvant therapy in patients with resectable disease [5,6]. In our prior series of 74 patients with unresectable pancreatic cancer treated with gemcitabine and radiotherapy, 11 patients (15%) achieved a CT detected partial response by RECIST, and no one achieved a complete response [4]. Additionally, the median time to CT detected partial response was 4.5 months from the start of radiation (range 1.6-19.1 months). This timing would not be useful for making clinical decisions. Histopathologically, pancreatic cancer is characterized by a prominent desmoplastic reaction [7]. This large amount of connective tissue would not be expected to regress after therapy and likely contributes to the frequent misinterpretation of scans.

Diffusion-weighted MRI (dMRI) has the potential to overcome the weaknesses of CT imaging in patients with pancreatic cancer. Diffusion-weighted imaging is a pulse sequence (utilizing Echo Planar imaging or EPI sequence) that can measure the mobility of water molecules within tissue at the cellular level [8]. The diffusion of water in tissue can be expressed as the apparent diffusion coefficient (ADC) which reflects overall diffusivity, and is dependent on many factors, including water mobility in intra- and extracellular spaces, the relative volume of these spaces, cellular membrane integrity, macromolecular components and permeability [9]. ADC values have been correlated with tumor cellularity in patients [10]. Low ADC values are observed in dense and fibrotic tumors due to increased tissue cellularity and reduced extracellular volume. Conversely, high ADC values have been described within necrotic regions of tumors [11,12].

By distinguishing between necrotic and viable tumor, dMRI has the potential to detect and measure cellular changes that occur in response to successful therapies, such as chemoradiation. These changes would be expected to be detectable prior to macroscopic changes in mass, size or morphology since removal of tumor macromolecular debris occurs relatively slowly. In fact, clinical studies have shown that dMRI can predict tumor response often several months prior to detectable radiographic changes [13–18]. Therefore, we decided to study the effectiveness of dMRI to predict response in patients with pancreatic cancer receiving neoadjuvant chemoradiation therapy.

2. Methods

2.1. Patients

Patients with resectable pancreatic cancer planning to undergo neoadjuvant chemoradiation therapy were eligible for this study. Patients had to have no contraindications to MRI, adequate renal function, and no prior history of radiation therapy to the abdomen. All participating subjects signed informed consent. This protocol was approved by University of Michigan Institutional Review Board.

2.2. Study Procedures

After signing informed consent, patients underwent dMRI prior to starting neoadjuvant chemoradiation. The type of chemotherapy and

Table 1. Patient and tumor characteristics

Subject	Age	Stage	Response*	Pre ADC†	Post ADC†	Δ ADC	OS (mo)
1	52	pT2N1M0	III	152	171	19	22.4
2	59	pT3N1M0	III	162			44.8
3	59	pT3N1M0	III	168	122	-46	25.6
4	68	pT3N0M0	I	83	185	102	26.5
5	66	pT2N0M0	IIB	140			10.0
6	64	pT4NxM0		136			3.3
7	71	pT3N1M0	IIA	119	170	51	28.6
8	55	pT4NxM0		141	178	36	12.0
9	56	pTxNxM1		181	186	5	6.1
10	50	pT3N1M0	IIB	160	179	19	10.9

* Response Criteria, I: <10% tumor cell destruction, IIA: 10–50% tumor cell destruction, IIB: 51–90% tumor cell destruction, III: <10% viable appearing tumor cells present.
† Mean tumor ADC, units $\times 10^{-5}$ mm^2/s determined using b values 0, 100, 500, 800 s/mm^2.

dose of radiation was not specified in the study protocol; however, most of the patients were enrolled on an unrelated clinical trial and received gemcitabine (1000 mg/m^2 on days 1, 8, and 15) plus oxaliplatin (85 mg/m^2 on days 1 and 15) with 30 Gy in 2 Gy fractions.

2.3. Diffusion MRI

MRI scans included a fat saturated gradient recalled echo T1-weighted sequence (without and with gadolinium), a fat-saturated fast spin-echo T2-weighted sequence, a single shot fast spin-echo T2-weighted sequence, a T1-weighted fat suppressed SPGR, and a diffusion sequence. The diffusion weighted technique was single shot diffusion weighted echo-planar with spectral selective fat suppression, with transaxial slices performed in three orthogonal diffusion directions over a range of b-values (0, 100, 500, and 800 s/mm^2). The same MRI scanner was used for all patients on the study. All images were obtained with multiple slices to cover the entire tumor volume. The tumor volume, also known as the region of interest, was determined by consensus between an abdominal MR radiologist (H.H.) and the primary investigator (K.C.C.). ADC maps were generated using software created by the University of Michigan (T.L.C., B.D.R., C.J. G., A.R.). Histograms and median/mean ADC values were determined for each scan.

2.4. Endpoints

The primary objective of the study was to correlate tumor ADC levels and distributions with pathologic and CT response. Pathologic response was graded according to the system developed by Evans [19]. A single pathologist (J.K.G.) graded each specimen based on the percent of tumor cell destruction. CT response was based on the change in product of the two largest tumor diameters. A secondary objective was to correlate overall survival with pretreatment and post-treatment ADC parameters.

2.5. Statistical Analysis

Histograms depicting the distribution of voxels within a tumor were extracted from ADC maps which were generated from dMRI images. The median and mean ADC values for each histogram/tumor were determined using Excel Software (Microsoft). Pathologic response grading was converted to numerical values of tumor cell destruction as follows Grade I 5%, Grade IIA 30%, Grade IIB 70%, Grade III 95%. Pearson correlation coefficient was calculated to describe the relationship between ADC and percent tumor cell destruction. Student's t test was used to compare mean ADC values

A

ROI with Low ADC

B

ROI with High ADC
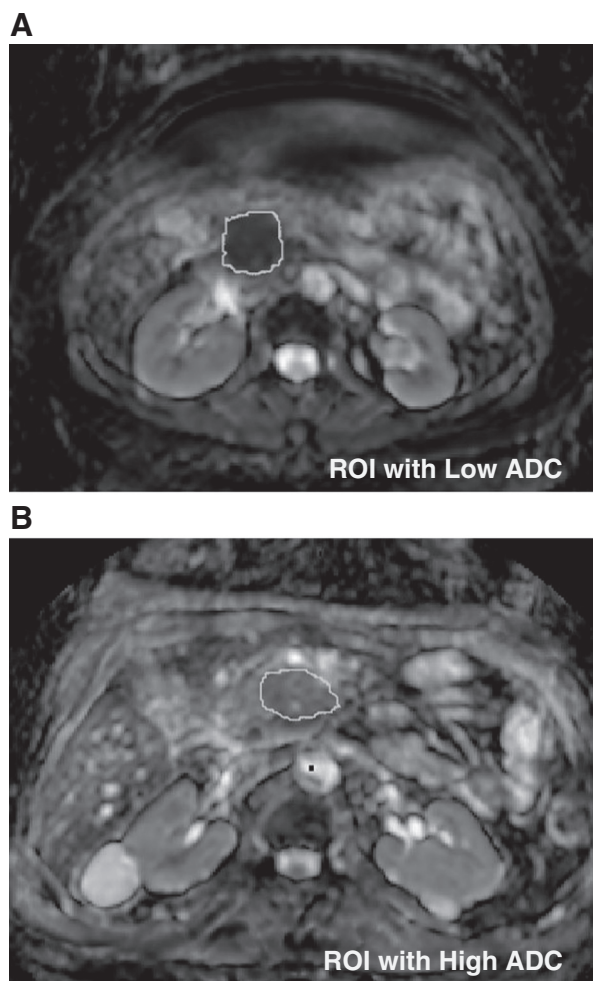
Figure 1. ADC maps obtained from patients on the study. The region of interest (tumor) is outlined. Representative tumors with a low (A, 119×10^{-5} mm^2/s) and high (B, 168×10^{-5} mm^2/s) mean ADC are shown.

and changes in size on CT scans between groups. A *P* value of ≤ .05 was considered statistically significant.

3. Results

3.1. Patient Population and Study Interventions

Between October 2008 and December 2009 we performed a study of dMRI in patients undergoing neoadjuvant chemoradiation for pancreatic cancer. Sixteen patients consented to the study. Four of the patients did not have imaging due to the inability to undergo MRI or the development of metastases prior to starting therapy. Out of the twelve remaining patients, 10 had surgery, one developed metastasis during treatment, and one passed away prior to surgery. Out of the patients who went to surgery, three were found to be unresectable at the time of their operation and seven patients successfully underwent pancreaticoduodenectomy.

The median time from the pretreatment dMRI to the start of chemoradiation was 3.5 days (range, 1–63). Pathologic response measured as percent tumor cell destruction was graded by a pathologist (JKG) (Table 1). There was one Grade I response (>90% viable tumor), one Grade IIA response (11–50% tumor cell destruction), two Grade IIB responses (51–90% tumor cell destruction), and three Grade III responses (minimal viable tumor).
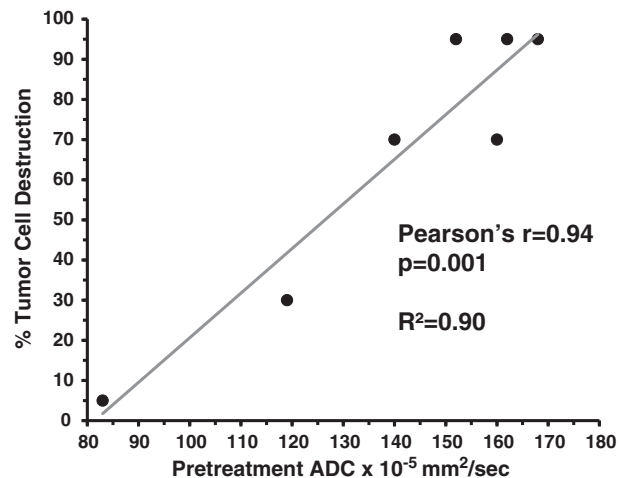
Figure 2. Relationship between pretreatment mean tumor ADC and subsequent histopathologic response after chemoradiation therapy. The percentage of tumor cell destruction was converted from the grading system described by Evans DB *et al.* (19) to a numerical scale. Pearson correlation coefficient was calculated to describe the relationship between ADC and percent tumor cell destruction.

### 3.2. Correlation of ADC Parameters and Tumor Response

We determined the mean ADC for each tumor prior to treatment with neoadjuvant chemoradiation. The mean pretreatment ADC for the entire group was 144.2×10^{-5} mm^2/s (SD 27.9). Representative images of a tumor with a low ADC value and a high ADC value are shown in Figure 1. There was a significant direct linear correlation between pre-treatment ADC and percent tumor cell destruction with a Pearson's r coefficient of 0.94 (*P* = .001) and an R^2 value of 0.90 (Figure 2). Analysis on ADC histograms for each tumor further demonstrated that tumors with increased tumor cell destruction from chemoradiotherapy were shifted towards higher ADC values (Figure 3). ADC histograms were approximately 150×10^{-5} mm^2/sec in width for each tumor. The tumors with the least amount of cellular destruction after chemoradiation demonstrated a high degree of restricted diffusion at baseline or low ADC values. Responsive tumors had mean ADCs above 150×10^{-5} mm^2/s with a minimal amount of voxels below an ADC of 100×10^{-5} mm^2/sec.

Mean pretreatment ADC was significantly higher in patients who had a pathologic response defined as minimal (<10%) viable tumor (ADC 161×10^{-5} mm^2/s +/− 5, n = 3) compared to patients with a poor pathologic response (ADC 125×10^{-5} mm^2/s +/− 16, n = 4). In contrast, there was no significant change in tumor size seen on CT imaging obtained prior to and after chemoradiation in responding or non-responding patients (Figure 4).

3.3. Relationship of Tumor Cell Destruction and ADC with Survival

Patients who had >90% tumor cell destruction (Grade III response) had a median survival of 25.6 months, whereas patients who had greater than 10% viable tumor remaining (Grade I-IIB response) after chemoradiation had a median survival of 18.7 months. Patients with unresectable tumors had a median survival of 6.1 months. All patients with a mean pretreatment tumor ADC of <145 had either viable tumor remaining after chemoradiation or were unresectable. Three of the five patients with an ADC >145 x 10^{-5} mm^2/s underwent surgery and were found to have minimal viable tumor remaining after chemoradiation.

A

B
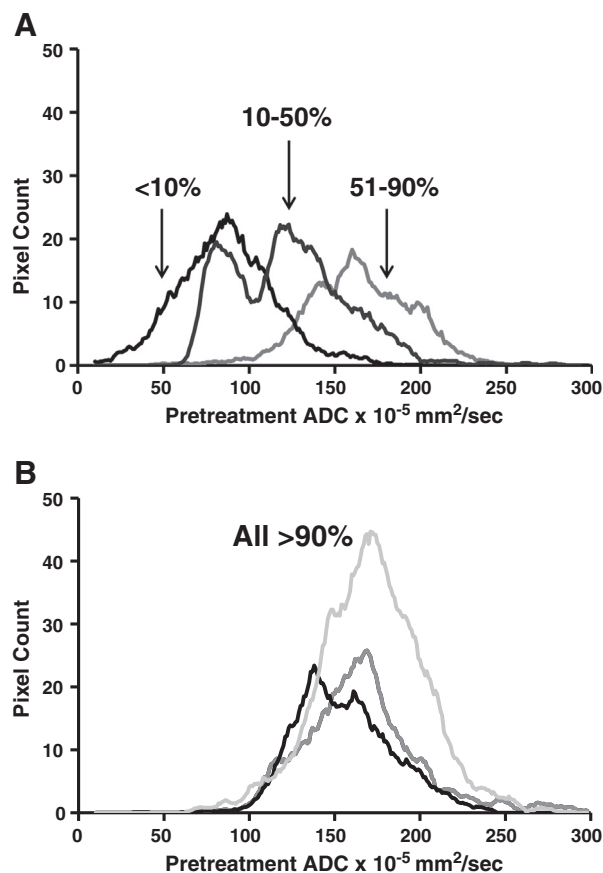
Figure 3. Pretreatment ADC histograms generated for each tumor with the corresponding amount of tumor cell destruction (percentage listed) seen after chemoradiation therapy and surgical resection. A shift towards a higher ADC value was associated with improved pathologic response to chemoradiation.

3.4. Effect of Metal Biliary Stent on Diffusion Weighted Sequences

Due to the high prevalence of metal biliary stents in our patient population and the potential artifact on diffusion weighted sequences, we tested three metal biliary stents to determine the feasibility of including these patients on dMRI studies. Two nitinol (nickel titanium alloy) MRI compatible stents were compared to a standard stainless steel stent in a water phantom to determine the amount of artifact seen with different MRI sequences. Considerable artifact was seen in the diffusion sequence with the stainless steel stent but not in the nitinol containing stents (Figure 5). Mean maximum radial distortion on dMRI scans was 3.4 mm and 3.8 mm in the nitinol containing stents versus 11.8 mm in the stainless steel stent. Additionally, the nitinol containing stents produced minimal torque in T2 or diffusion weighted sequences.

4. Discussion

In the current study, we found an association between pretreatment tumor ADC values and subsequent tumor response to chemoradiation in patients with pancreatic cancer. There was a significant correlation between pre-treatment mean tumor ADC values and the percent tumor cell destruction observed at the time of surgery. Additionally, analysis of pretreatment ADC histograms for each tumor demonstrated a shift towards higher ADC values in tumors that later responded to treatment. These preliminary findings suggest dMRI may be useful as an imaging biomarker in pancreatic cancer.

An early imaging biomarker for patients with pancreatic cancer is greatly needed. Treatment with chemoradiation is associated with considerable toxicity and a poor outcome for many patients [1,20,21]. By identifying either before treatment or part way into a treatment course if a patient is responding, we have the potential to adapt therapy. Patients with nonresponding tumors can have therapy intensified or modified. Additionally, dMRI could be useful to determine if patients are resectable after chemoradiation therapy. For patients who are borderline resectable, it is likely some become resectable after chemoradiation but are never offered surgery because pancreatic tumors regress slowly on CT imaging [2–6]. Although longitudinal dMRI was not accomplished in this study, additional information related to spatially varying ADC changes within the tumor mass could be obtained after initiation of treatment to provide information related to tumor response and identify patients who may be resectable despite what is seen on CT [18].

A limited number of reports have looked at dMRI in pancreatic cancer. One retrospective study found tumors with low ADC values at baseline responded poorly to systemic therapy, consistent with our findings [22]. Another report found a correlation between preoperative ADC values and the amount of tumor fibrosis in patients who did not receive preoperative therapy. Tumors with a low ADC were found to be densely fibrotic [23]. The large amount of fibrotic tissue in pancreatic tumors may limit the delivery of radiosensitizing systemic therapy and lower the amount of oxygen available for radiation induced free radical formation thereby decreasing the effectiveness of chemoradiation therapy [24].

Abdominal dMRI has several challenges compared to other sites such as the brain or breast. Respiratory motion and organ movement can lead to considerable distortion artifact and can make image registration a challenge. The pancreas poses an added barrier due to the increasing utilization of metal biliary stents. Metal stents are preferred over plastic stents due to lower occlusion and complication rates [25]. Recently, multiple companies have developed MRI compatible metal stents using a nickel titanium alloy (nitinol). We compared the artifact from a standard stainless steel stent to two nitinol containing stents in a water phantom. The stainless steel stent produced considerable streak artifact which would make the interpretation and determination/quantification of ADC values difficult. Additionally, it is unknown if stainless steel stents are safe in patients undergoing MRI. The two nitinol stents we tested are marketed as MRI compatible and produced minimal artifact on diffusion-weighted sequences. This finding allows for the potential inclusion of patients with nitinol containing biliary stents on future studies examining dMRI.

There are several limitations to our study including the small number of patients and the endpoints examined. This study was designed as a feasibility study to demonstrate dMRI can be used in patients with pancreatic cancer undergoing chemoradiation. It was not powered to determine if diffusion metrics could be used to predict subsequent survival. Our primary endpoint was pathologic response according to the grading system developed by Evans et al. [19]. This system has been utilized in prior studies and is shown to correlate with patient outcome [19,26]. Larger studies will be required to determine if dMRI is useful as a prognostic marker for early treatment response stratification of patients with pancreatic cancer.

In conclusion, the use of dMRI in the management of patients with pancreatic cancer has several exciting potential applications. In our study we found a correlation between pretreatment mean ADC
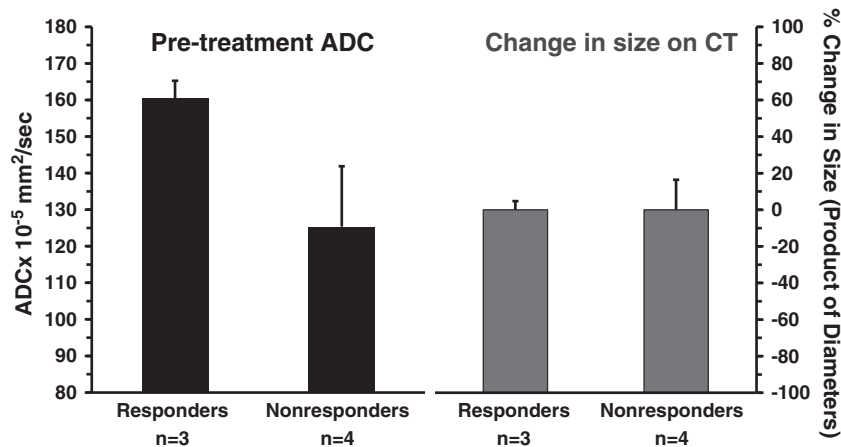
Figure 4. Comparison of pretreatment ADC and change in size on CT scan in patients showing a pathologic response (>90% tumor cell destruction) and in nonresponding patients (>10% viable tumor). Mean pretreatment tumor ADC was significantly higher in responding patients compared to nonresponding patients. Whereas, tumor size did not change on CT imaging after treatment with neoadjuvant chemoradiation.
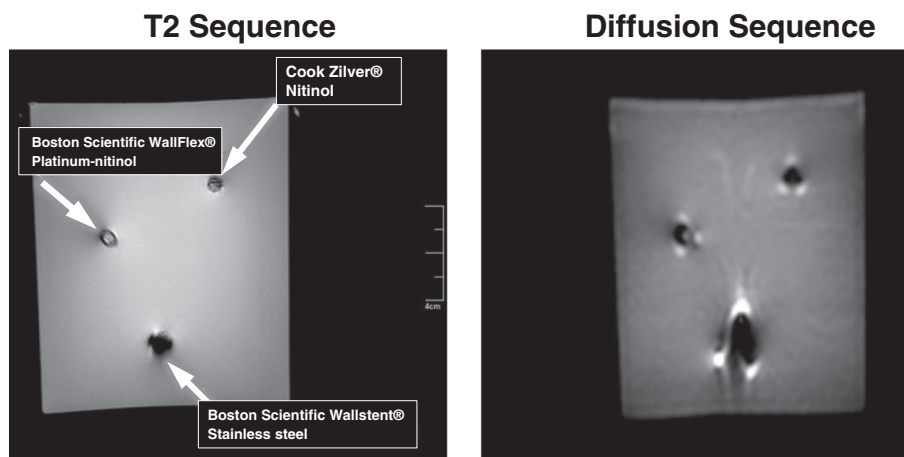
Figure 5. One stainless steel and two nitinol (nickel titanium alloy) stents were placed in fixed diameter plastic cylinders to simulate a bile duct. Stents were scanned in a water phantom with T2 and diffusion weighted MRI sequences. High levels of artifact were seen in the diffusion sequence with the stainless steel stent but not with the nitinol containing stents.

values and subsequent tumor response. Larger studies examining the utility of this imaging modality as an early response biomarker in patients with pancreatic cancer are underway at our institution.

Conflict of Interest Statement

The authors have no conflicts of interest to report.

References

[1] National Comprehensive Cancer Network. *Clinical Practice Guidelines in Oncology: Pancreatic Adenocarcinoma* (Version 1.2013). Accessed 10/18/2013 www.nccn.org.

[2] Kim HJ, Czischke K, Brennan MF, and Conlon KC (2002). Does neoadjuvant chemoradiation downstage locally advanced pancreatic cancer? *J Gastrointest Surg* **6**(5), 763–769.

[3] Moutardier V, Magnin V, Turrini O, Viret F, Hennekinne-Mucci S, Goncalves A, Pesenti C, Guiramand J, Lelong B, and Giovannini J, et al (2004). Assessment of pathologic response after preoperative chemoradiotherapy and surgery in pancreatic adenocarcinoma. *Int J Radiat Oncol Biol Phys* **60**(2), 437–443.

[4] Murphy JD, Adusumilli S, Griffith KA, Ray ME, Zalupski MM, Lawrence TS, and Ben-Josef E (2007). Full-dose gemcitabine and concurrent radiotherapy for unresectable pancreatic cancer. *Int J Radiat Oncol Biol Phys* **68**(3), 801–808.

[5] Desai SP, Ben-Josef E, Lawrence TJ, Francis IR, Greenson JK, Alfred CE, Colletti LM, Simeone DM, Normolle DP, and Zalupski MM (2006). A phase I study of oxaliplatin, full-dose gemcitabine and concurrent radiation therapy in patients with pancreatic cancer. *J Clin Oncol* **24**(18), 204s.

[6] Mornex F, Girard N, Delpero JR, and Partensky C (2005). Radiochemotherapy in the management of pancreatic cancer – Part I: Neoadjuvant treatment. *Semin Radiat Oncol* **15**(4), 226–234.

[7] Mahadevan D and Von Hoff DD (2007). Tumor-stroma interactions in pancreatic ductal adenocarcinoma. *Mol Cancer Ther* **6**(4), 1186–1197.

[8] Lebihan D, Turner R, Douek P, and Patronas N (1992). Diffusion MR imaging – clinical applications. *Am J Roentgenol* **159**(3), 591–599.

[9] Lebihan D, Breton E, Lallemand D, Grenier P, Cabanis E, and Lavaljeantet M (1986). MR imaging of Intravoxel incoherent motions – application to diffusion and perfusion in neurologic disorders. *Radiology* **161**(2), 401–407.

[10] Sugahara T, Korogi Y, Kochi M, Ikushima I, Shigematu Y, Hirai T, Okuda T, Liang LX, Ge YL, and Komohara Y, et al (1999). Usefulness of diffusion-weighted MRI with echo-planar technique in the evaluation of cellularity in gliomas. *J Magn Reson Imaging* **9**(1), 53–60.

[11] Brunberg JA, Chenevert TL, Mckeever PE, Ross DA, Junck LR, Muraszko KM, Dauser R, Pipe JG, and Betley AT (1995). In-vivo MR determination of water diffusion-coefficients and diffusion anisotropy - correlation with structural alteration in gliomas of the cerebral hemispheres. *Am J Neuroradiol* **16**(2), 361–371.

[12] Lang P, Wendland MF, Saeed M, Gindele A, Rosenau W, Mathur A, Gooding CA, and Genant HK (1998). Osteogenic sarcoma: noninvasive in vivo assessment of tumor necrosis with diffusion-weighted MR imaging. *Radiology* **206**(1), 227–235.

[13] Hamstra DA, Chenevert TL, Moffat BA, Johnson TD, Meyer CR, Mukherji SK, Quint DJ, Gebarski SS, Fan XY, and Tsien CI, et al (2005). Evaluation of the functional diffusion map as an early biomarker of time-to-progression and overall survival in high-grade glioma. *Proc Natl Acad Sci U S A* **102**(46), 16759–16764.

[14] Mardor Y, Pfeffer R, Spiegelmann R, Roth Y, Maier SE, Nissim O, Berger R, Glickman A, Baram J, and Orenstein A, et al (2003). Early detection of response to radiation therapy in patients with brain malignancies using conventional and high b-value diffusion-weighted magnetic resonance imaging. *J Clin Oncol* **21**(6), 1094–1100.

[15] Byun WM, Shin SO, Chang YM, Lee SJ, Finsterbusch J, and Frahm J (2002). Diffusion-weighted MR imaging of metastatic disease of the spine: Assessment of response to therapy. *Am J Neuroradiol* **23**(6), 906–912.

[16] Hayashida Y, Yakushiji T, Awai K, Katahira K, Nakayama Y, Shimomura O, Kitajima M, Hirai T, Yamashita Y, and Mizuta H (2006). Monitoring therapeutic responses of primary bone tumors by diffusion-weighted image: initial results. *Eur Radiol* **16**(12), 2637–2643.

[17] Uhl M, Saueressig U, van Buiren M, Kontny U, Niemeyer C, Koehler G, Ilyasov K, and Langer M (2006). Osteosarcoma - Preliminary results of in vivo assessment of tumor necrosis after chemotherapy with diffusion- and perfusion-weighted magnetic resonance imaging. *Invest Radiol* **41**(8), 618–623.

[18] Thoeny HC and Ross BD (2010). Predicting and monitoring cancer treatment response with diffusion-weighted MRI. *J Magn Reson Imaging* **32** (1), 2–16.

[19] Evans DB, Rich TA, Byrd DR, Cleary KR, Connelly JH, Levin B, Charnsangavej C, Fenoglio CJ, and Ames FC (1992). Preoperative chemoradiation and pancreaticoduodenectomy for adenocarcinoma of the pancreas. *Arch Surg* **127** (11), 1335–1339.

[20] Loehrer PJ, Feng Y, Cardenes H, Wagner L, Brell JM, Cella D, Flynn P, Ramanathan RK, Crane CH, and Alberts SR, et al (2011). Gemcitabine alone versus gemcitabine plus radiotherapy in patients with locally advanced pancreatic cancer: an eastern cooperative oncology group trial. *J Clin Oncol* **29**(31), 4105–4112.

[21] Chauffert B, Mornex F, Bonnetain F, Rougier P, Mariette C, Bouche O, Bosset JF, Aparicio T, Mineur L, and Azzedine A, et al (2008). Phase III trial comparing intensive induction chemoradiotherapy (60 Gy, infusional 5-FU and intermittent cisplatin) followed by maintenance gemcitabine with gemcitabine alone for locally advanced unresectable pancreatic cancer. Definitive results of the 2000-01 FFCD/SFRO study. *Ann Oncol* **19**(9), 1592–1599.

[22] Niwa T, Ueno M, Ohkawa S, Yoshida T, Doiuchi T, Ito K, and Inoue T (2009). Advanced pancreatic cancer: the use of the apparent diffusion coefficient to predict response to chemotherapy. *Br J Radiol* **82**(973), 28–34.

[23] Muraoka N, Uematsu H, Kimura H, Imamura Y, Fujiwara Y, Murakami M, Yamaguchi A, and Itoh H (2008). Apparent diffusion coefficient in pancreatic cancer: characterization and histopathologican correlations. *J Magn Reson Imaging* **27**(6), 1302–1308.

[24] Olson P and Hanahan D (2009). Breaching the cancer fortress. *Science* **324** (5933), 1400–1401.

[25] Davids PHP, Groen AK, Rauws EAJ, Tytgat GNJ, and Huibregtse K (1992). Randomized trial of self-expanding metal stents versus polyethylene stents for distal malignant biliary obstruction. *Lancet* **340**(8834–5), 1488–1492.

[26] Chatterjee D, Katz MH, Rashid A, Varadhachary GR, Wolff RA, Wang H, Lee JE, Pister PWT, Vauthey JN, and Crane C (2012). Histologic grading of the extent of residual carcinoma following neoadjuvant chemoradiation in pancreatic ductal adenocarcinoma. *Cancer* **118**(12), 3182–3190.